



## Biogenic Synthesis of Silver Nanoparticles Using *Onosma Bourgaei* Leaves: Characterization and Antioxidant Activity

Ramazan Erenler<sup>1,2\*</sup>, Esmâ Nur Gecer<sup>2</sup>

<sup>1</sup>Research Laboratory Practice and Research Center, Iğdir University, 7600, Türkiye

<sup>2</sup>Department of Chemistry, Arts and Sciences Faculty, Tokat Gaziosmanpaşa University, 60250 Tokat, Türkiye

Received: 30 June 2024; Revised: 07 August 2024; Accepted: 07 August 2024

\*Corresponding author e-mail: [renler@gmail.com](mailto:renler@gmail.com)

**Citation:** Erenler, R.; Geçer, E. N., *Int. J. Chem. Technol.* 2024, 8(2), 98-104.

### ABSTRACT

Green synthesis of nanoparticles has achieved substantial significance recently owing to its application in many fields. The silver nanoparticle synthesis (OB-AgNPs) was accomplished using *Onosma bourgaei*. Spectroscopic methods were utilized to elucidate the structure of synthesized OB-AgNPs. UV/Vis analysis displayed the absorption at 450 nm. The functional groups were assigned by FTIR. The morphology was presented by SEM and TEM analysis and particles were determined to have a spherical shape. The XRD analysis (2 $\theta$ ) [111, 200, 220, 311, and 222] displayed the face-centered cubic structure of the particle. The particle magnitude of the nanoparticle was established to be 16.3 nm by the Scherrer formula. The zeta potential was defined as -46.1 mV, indicating high stability. Antioxidant activity was conducted using the FRAP, DPPH<sup>•</sup>, and ABTS<sup>•+</sup> assays. OB-AgNPs showed the outstanding ABTS<sup>•+</sup> scavenging effect (2.92, IC<sub>50</sub>) compared with the standard BHT (7.17, IC<sub>50</sub>,  $\mu\text{g/mL}$ ).

**Keywords:** *Onosma bourgaei*, natural products, silver nanoparticles, green chemistry, antioxidant effect.

### 1. INTRODUCTION

Nanotechnology has recently gained outstanding interest thanks to its large variety of functions.<sup>1-6</sup> Noble metals have been usually employed for the NPs synthesis. Along with the noble metallic NPs, silver nanoparticles (AgNPs) have a wide variety of commercial purposes including optics, electronics, catalysis, sensors, and medicine.<sup>7-11</sup> Some physicochemical procedures such as electrochemical, photochemical, and radiation are commonly used to produce AgNPs. However, these methods lead to environmental pollution and toxic residues in the nanoparticles. Natural products attract considerable attention for the synthesis of AgNPs.<sup>12-14</sup> Medicinal plants, algae, microorganisms, vegetable wastes, oilcake, panchakavya, seaweeds, and enzymes have been used for the synthesis of AgNPs.<sup>15-16</sup> After the advancement of spectroscopic analysis in the 19<sup>th</sup> century, bioactive compounds named secondary metabolites in the plant began to be elucidated.<sup>16-21</sup> Hence, plants became the focus of scientific attention, and lots of compounds used in drug discovery were isolated and identified.<sup>22-26</sup> Moreover, natural

compounds inspired synthetic chemists to synthesize these compounds.<sup>27-32</sup>

*Onosma* genus (Boraginaceae) consists of 230 species, mainly spread through the Mediterranean area, and Europe. This genus has about 103 species in Turkey flora.<sup>33</sup> The compounds from species of this genus include alkannin, flavonoids, ferulic acid, vanillic acid, alkaloids, lipids, shikonin derivatives, and naphthoquinone derivatives. *Onosma* genus was reported to reveal considerable biological effects including anti-inflammatory, wound healing, antibacterial, palliative, antioxidant, and anticancer effects.<sup>34</sup> This genus is commonly used for traditional medicine against rheumatism, bladder pain, kidney inflammation, and heart palpitations. It is also employed in the remedy of hypertension, fever, infectious diseases, pain relief, wounds, and bites.<sup>35</sup> Consequently, AgNPs capped and stabilized by the natural compounds of *Onosma bourgaei* are expected to be effective for food and medicinal applications.

Reactive oxygen species (ROS) called free radicals, containing singlet oxygen, peroxy, superoxide, nitric oxide, and hydroxyl radicals may cause severe cellular damage that transforms into diseases.<sup>36</sup> ROS could give rise to DNA damage, cancer, and cardiovascular diseases. While various metabolic tasks generate ROS, they can be inhibited or retarded by bioactive compounds that exist in plants.<sup>37-39</sup> Thus, the synthesis of antioxidant nanoparticles from corresponding plants is critical to understanding their health benefits.

Herein, green synthesis of OB-AgNPs was accomplished from *O. bourgaei* and the antioxidant activity of extract and synthesized nanostructure was performed.

## 2. EXPERIMENTAL

### 2.1. Materials

#### 2.1.1. Chemicals

All chemicals and solvents were bought from Sigma-Aldrich company, Steinheim, Germany.

#### 2.1.2. Plants

During the flowering season, *Onosma bourgaei* was collected at Tokat Gaziosmanpasa University Campus, and defined by Prof. Dr. Ozgur Eminagaoglu by comparison of the same sample deposited in the herbarium (ARTH-5600).

### 2.2. Methods

#### 2.2.1. Green synthesis of *O. bourgaei* (OB)

The air-dried *Onosma bourgaei* Boiss. leaves (10.0 g) were extracted in deionized (DI) water (120 mL) at room temperature for 24 hours. After filtration, half of the solution (50 mL) was subjected to reduced pressure to obtain extract (0.3 g). Half of the other solution (50 mL) was treated with AgNO<sub>3</sub> (0.1 mM, 100 mL) at 50°C for 3 hours to produce OB-AgNPs. When the addition of AgNO<sub>3</sub> solution was completed, the color turned from pale to brown indicating the silver ions reduction to form OB-AgNPs. The centrifugation was applied for 10 min at 5000 rpm once the mixture approached to room temperature. Afterward, the products in eppendorf were combined and then washed thoroughly with DI, and dried with freeze-drying.

#### 2.2.2. Characterization

OB-AgNPs structure was fully characterized by spectroscopic study. UV-Vis spectrophotometer (Hitachi U-2900) was used for the determination of the absorption spectrum. FTIR (Jasco 4700) analysis disclosed the functional groups of compounds in *O. bourgaei* extract. The stability of nanoparticles was determined by a Zetasizer Nano ZSP (Malvern, UK). XRD pattern was determined by diffractometer (Panalytical). SEM and TEM images demonstrated the morphology of OB-AgNPs. Micro analysis was measured by EDX detector.

#### 2.2.3. DPPH<sup>•</sup> Assay

DPPH assay was employed for the antioxidant activity of both nanoparticles and extract.<sup>40</sup> In brief, extract and OB-AgNPs were reacted with DPPH<sup>•</sup> radical (1 mL, 0.26 mM) at rt for 30 min. The IC<sub>50</sub> values demonstrated the concentration of both samples that scavenged 50% of the DPPH<sup>•</sup>. The Equation (Eq. 1) was employed for calculation of DPPH activity.

DPPH<sup>•</sup> scavenging activity (%) =  $[(X_1 - X_2) / X_1] \times 100$  (1).

The control and sample absorbances were indicated by X<sub>1</sub> and X<sub>2</sub> respectively. The results were stated as IC<sub>50</sub>.

#### 2.2.4. ABTS Assay

The activity of OB-AgNPs and leaves extract was tested using ABTS radical cation assay.<sup>41</sup> The reaction of ABTS (2.0 mM) with potassium persulfate for 6 hours at rt in the dark resulted in the ABTS<sup>•+</sup> solution. Sodium phosphate buffer was used to fix the absorbance at 734 nm (0.1 mM, pH 7.4). ABTS<sup>•+</sup> was then applied to the extract and nanoparticle solutions (3.0 - 50 µg/mL, 3 mL) (1.0 mL). The same equation used in the DPPH assay was used to calculate ABTS<sup>•+</sup> activity.

#### 2.2.5. Reducing power

The extract and OB-AgNPs solution (0.1 mL, 50-150 µg/mL) were reacted with K<sub>3</sub>Fe(CN)<sub>6</sub> (1.25 mL), and phosphate buffer, followed by a 25-minute incubation at 55°C. The reaction flask was vortexed for 3 minutes after the addition of CCl<sub>3</sub>COOH (1.25 mL) and FeCl<sub>3</sub> (0.25 mL), and the absorbance measurement was performed (700 nm).<sup>42</sup>

#### 2.2.6. Statistical Analysis

The biological activity results were stated as mean value and standard deviation of three independent assay. One-way ANOVA followed by Tukey's test were carried out to analyze the degree of variance using GraphPad Prism (8.0.1) at p < 0.05.

## 3. RESULTS and DISCUSSION

### 3.1. *O. bourgaei*-mediated Synthesis of Silver Nanoparticles

The synthesis of nanostructure was achieved using *O. bourgaei* leaves. In silver nanoparticles synthesis, UV measurements is an important evidence for proofing of nanostructure.<sup>43</sup> The colour change takes place due to the reduction of silver ions (Ag<sup>+</sup>) to the silver salt (Ag<sup>0</sup>). In this study, the maximum absorption was attained at 450 nm, presenting the product. (Figure 1).

The mechanism of formation of OB-AgNPs is shown in Figure 2; in which silver ions were reduced by the compounds in the *O. bourgaei* leaves extract. The synthesis of OB-AgNPs can take place by the stages of ion reduction, clustering and successive development of the product. Since the luteolin 7-glucoside is the major compound of *O. bourgaei*, reaction mechanism was demonstrated with this molecule.<sup>44</sup>

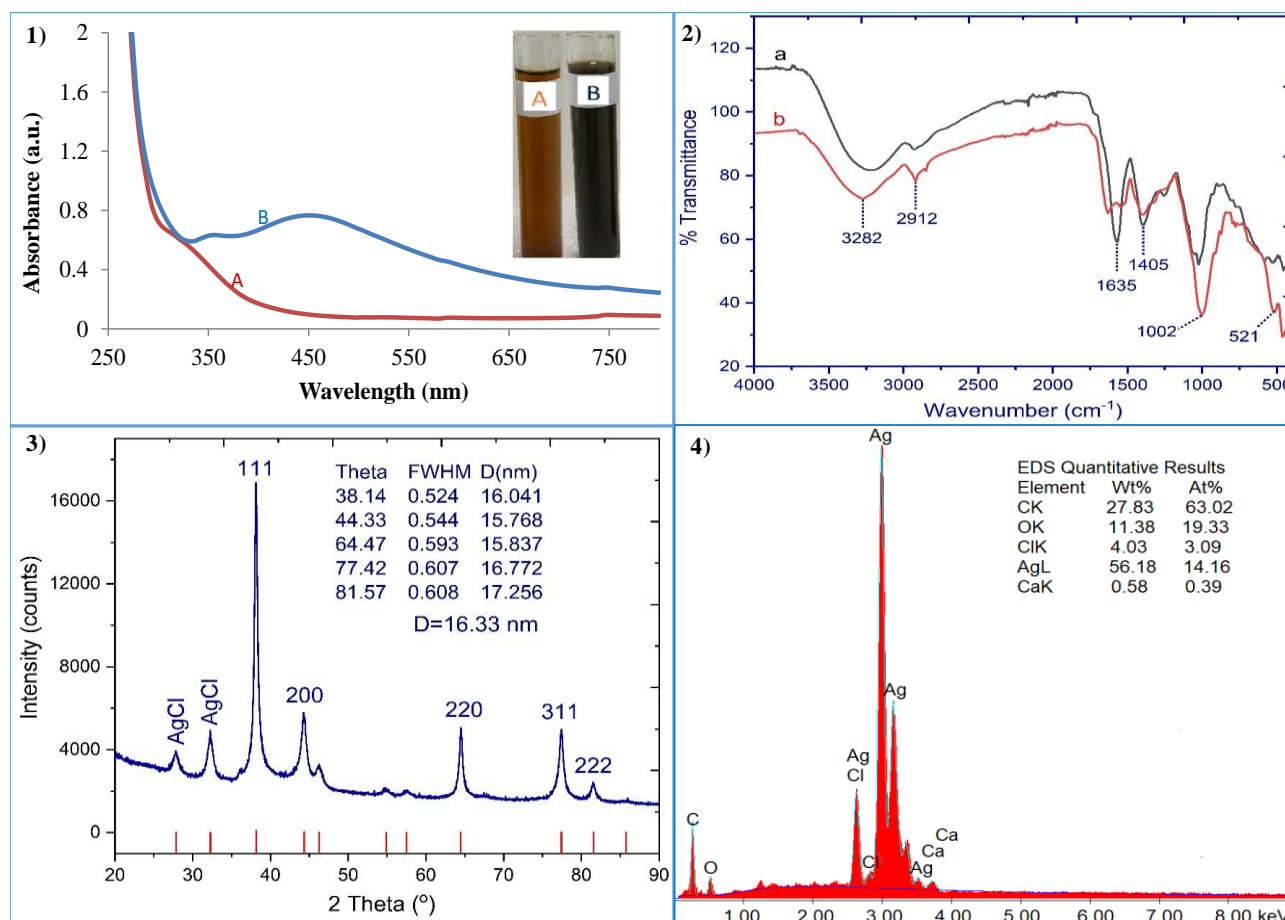


**Figure 1.** UV-Vis spectrum (1), FTIR spectrum of extract (a), nanoparticles (b) (2), XRD pattern (3), and EDX spectrum (4) of OB-AgNPs.

### 3.2. FTIR analysis

The functional groups of the molecules were displayed by FTIR analysis (Figure 1). A signal at  $3274\text{ cm}^{-1}$  indicated the characteristic hydroxyl group in the FTIR spectrum. The peak at  $2918\text{ cm}^{-1}$  can be ascribed to the C-H stretching bond. The signal observed at  $1632\text{ cm}^{-1}$  could be thanks to the carbon-carbon double bond stretching of alkene. The peaks at  $1396\text{ cm}^{-1}$  and  $1002\text{ cm}^{-1}$  could belong to the O-H bending of alcohol and the carbon-carbon double bond of alkene respectively. The silver oxide signals were observed at  $518\text{ cm}^{-1}$  and  $462\text{ cm}^{-1}$  which agreed with the reported study.<sup>45</sup>

### 3.3. XRD analysis

The XRD spectrum revealed the crystalline shape of OB-AgNPs.<sup>46</sup> The diffraction peaks ( $2\theta$ ) at  $38.15^\circ$ ,  $44.33^\circ$ ,  $64.48^\circ$ , and  $77.43^\circ$  corresponded to face-centered cubic structures with the facet of (1 1 1), (2 0 0), (2 2 0), and (3 1 1), respectively (Figure 1). The insignificant additional peaks in the XRD spectrum may correspond to the organic compounds.<sup>47</sup> The average crystalline size was calculated by the Scherrer Equation (Eq. 2)

$$D = 0.9 \lambda / \beta \cos \theta \quad (2)$$

In which,  $D$ ,  $\lambda$ ,  $\beta$  and  $\theta$  are average crystalline size ( $\text{\AA}$ ), x-ray wavelength (nm), angular line with at half maximum intensity (radians), Bragg angle (degree) respectively. The particle size was calculated as 16.3 nm by Scherrer equation.

### 3.4. SEM and TEM analyses

SEM and TEM images revealed the morphology of green synthesized OB-AgNPs, and the results clearly revealed spherical shaped of OB-AgNPs with an average particle size of 18.9 nm (Figure 3). In the formation of nanoparticles, the compounds in *O. bourgaei* leaf extract acted as a reducing agent. The elemental composition of OB-AgNPs was determined using a SEM equipped with an EDX detector. The energy-dispersive X-ray analysis revealed a strong signal in the Ag zone, which supported the formation of OB-AgNPs (Figure 1). In addition, the elemental analysis revealed the nanoparticle formation. The absorption signal from silver nanocrystals was nearly 2.983 keV due to surface plasmon resonance.<sup>48</sup>

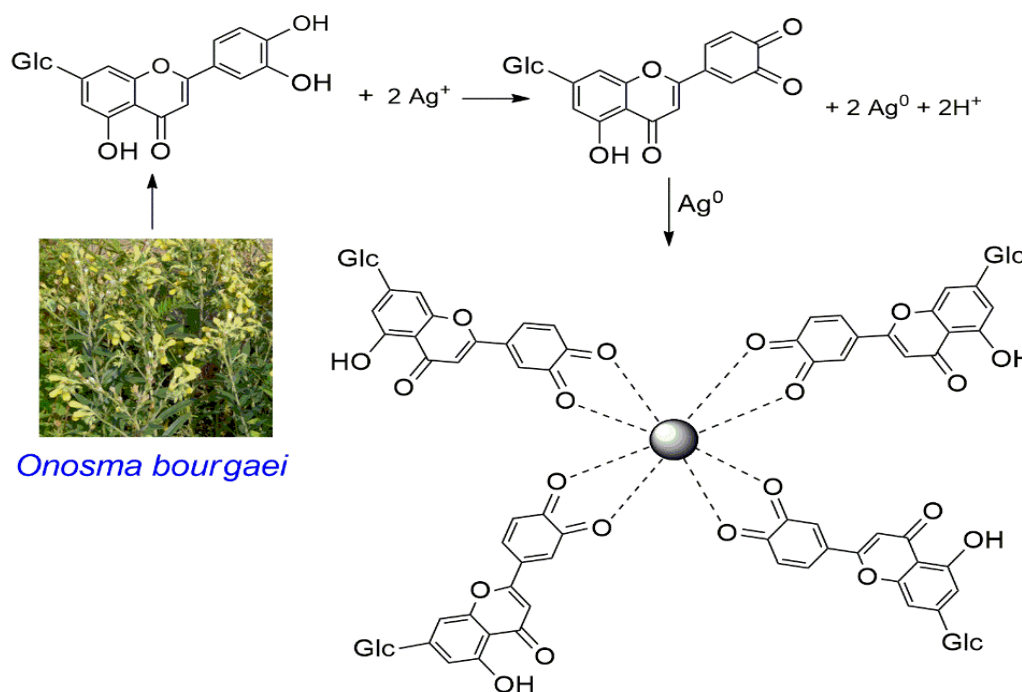


**Figure 2.** Possible reaction mechanism of synthesis of OB-AgNPs.

### 3.5. Zeta potential

When determining how much a particle interacts with other similarly charged particles, the zeta potential is essential.<sup>49</sup> The high negative value (-46.1 mV) of zeta potential disclosed the stability of nanoparticles. (Figure 4). Nanoparticles are stable in colloidal solution due to

electrostatic repulsion between negative charges. Furthermore, high negative values indicate anionic stability coordination. The negatively charged surfaces of OB-AgNPs enable nanoparticle aggregation to be avoided and their shape and size to be controlled.

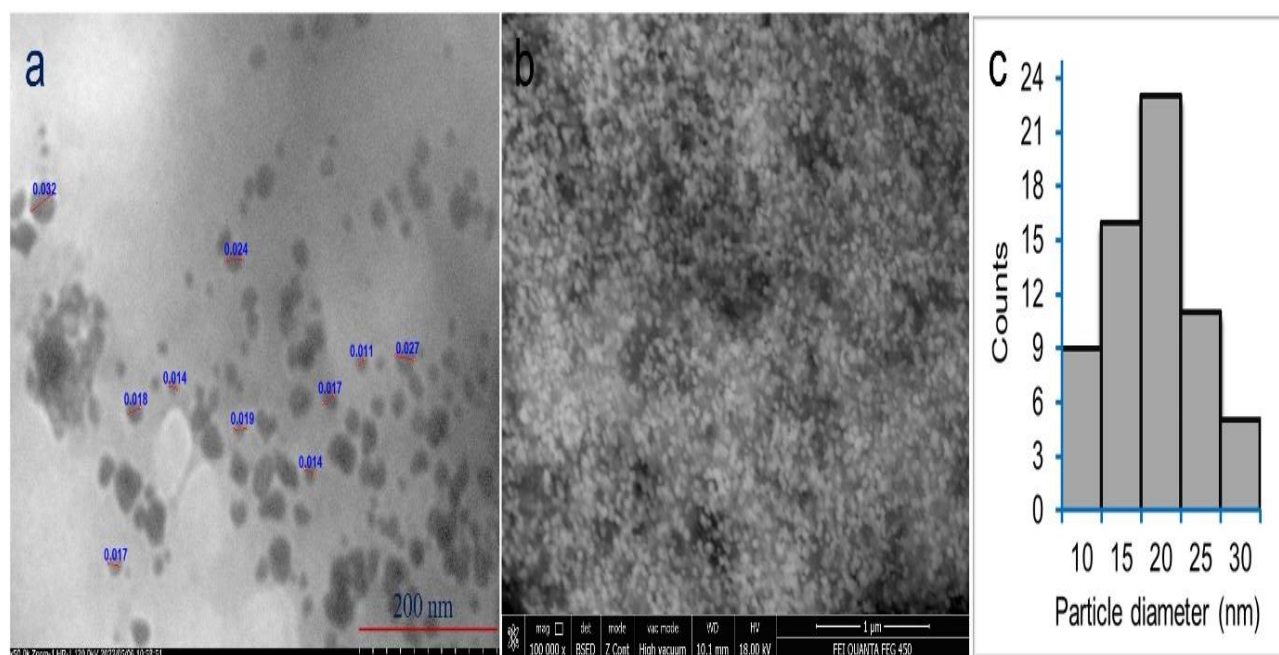


**Figure 3.** TEM (a), SEM (b) and particle size distribution (c) of OB-AgNPs.

### 3.6. Antioxidant activity

Antioxidant activity of OB-AgNPs and extract was performed using the DPPH, ABTS and FRAP assays (Figure 5). In the DPPH test, OB-AgNPs revealed a significantly higher activity than the extract with the values of  $8.14 \pm 0.13$  ( $IC_{50}$ ,  $\mu\text{g/mL}$ ) and  $12.17 \pm 0.72$  ( $IC_{50}$ ,  $\mu\text{g/mL}$ ) respectively. In addition, the activity of OB-AgNPs was determined to be higher than standard

BHT ( $10.78 \pm 0.093$ ,  $IC_{50}$ ,  $\mu\text{g/mL}$ ) as well. In concerning the ABTS radical cation test, the excellent activity of OB-AgNPs was observed ( $2.92 \pm 0.03$ ,  $IC_{50}$ ,  $\mu\text{g/mL}$ ) compared to extract ( $8.89 \pm 0.55$ ,  $IC_{50}$ ,  $\mu\text{g/mL}$ ) and standard Trolox ( $5.49 \pm 0.16$ ,  $IC_{50}$ ,  $\mu\text{g/mL}$ ). In FRAP assay, OB-AgNPs were observed to exhibit better activity than the extract.

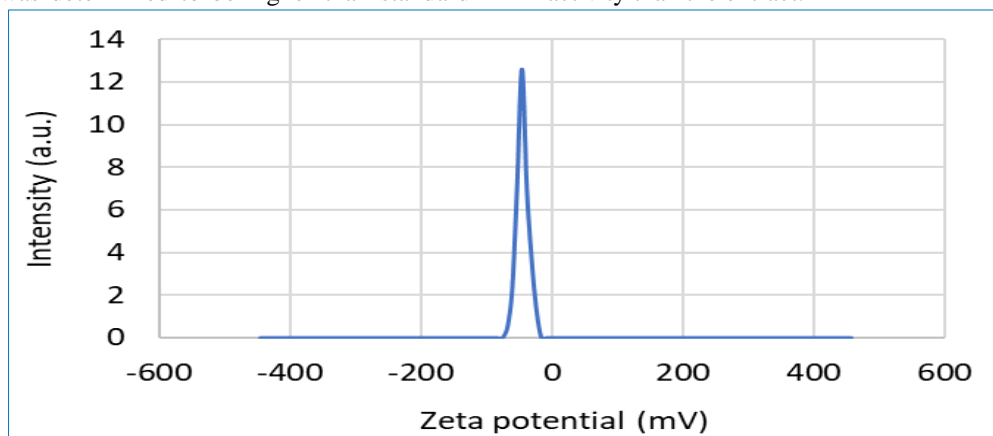


Figure 4. Zeta potential of OB-AgNPs.

Consequently, OB-AgNPs synthesized from *O. bourgaei* could be an excellent antioxidant agent. OB-AgNPs have the potential to be drugs in the treatment of diseases caused by free radicals. Further research should be performed on silver nanoparticles synthesized from *O. bourgaei* to display the corresponding effects. AgNPs synthesized from some plants exhibited antioxidant activity. Silver nanoparticles synthesized from *Sambucus nigra* leaves revealed the considerable

antimicrobial and antioxidant activity.<sup>50</sup> Moreover, *Sambucus ebulus* leaves extract was used for synthesis of silver nanoparticles and they displayed the good antioxidant activity.<sup>51</sup> Due to the incorporation of bioactive compounds from plants,<sup>52-55</sup> the silver nanoparticles capped, stabilized and reduced by the corresponding compounds displayed the biological activities.

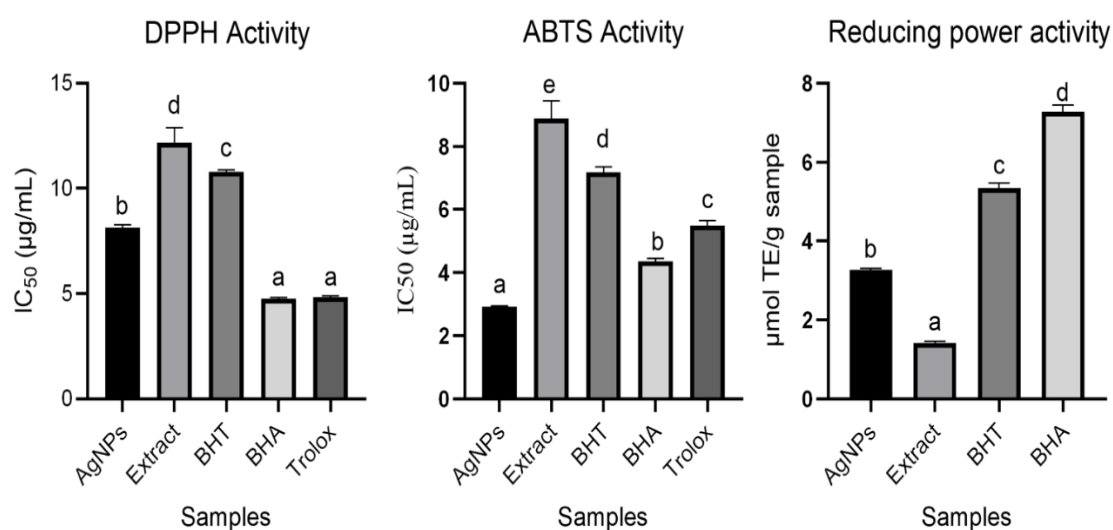


Figure 5. Antioxidant activity of extract and OB-AgNPs. Different letters indicated significantly different ( $p < 0.05$ ) compared in each assay.

#### 4. CONCLUSION

Silver nanoparticles were synthesized using *O. bourgaei* leaves in a facile, eco-friendly, and cost-effective method. The structure of green synthesized nanoparticles was elucidated by spectroscopic techniques. *O. bourgaei* has been employed in traditional medicine to treat various diseases. These effects were caused by the secondary metabolites that the plant contained. Due to the great advantage of nanostructure for medicine. The nanostructure capped bioactive compounds could be effective for the pharmaceutical and food industry.

#### Conflict of Interest

The authors declare that there is no competing interest.

#### REFERENCES

- Erenler, R.; Gecer, E. N.; Genc, N.; Yanar, D. Int J Chem Technol 2021, 5 (2), 141-146.
- Gecer, E. N. J Inorg Organomet Polym Mater 2021, 31 (11), 4402-4409.
- Genc, N. Particul Sci Technol 2021, 39 (5), 562-568.
- Genc, N.; Yildiz, I.; Chaoui, R.; Erenler, R.; Temiz, C.; Elmastas, M. Inorg Nano-Met Chem 2021, 51 (3), 411-419.
- Dag, B. Particul Sci Technol 2022, 40 (4), 512-520.
- Erenler, R.; Dag, B. Inorg Nano-Met Chem 2022, 52 (4), 485-492.
- Erenler, R.; Gecer, E. N. Turk J Agricul Food Sci Tech 2022, 10 (6), 1112-1115.
- Erenler, R.; Gecer, E. N. J Nano Res 2022, 75, 17-28.
- Gecer, E. N.; Erenler, R. Turk J Biodiv 2022, 5 (1), 50-56.
- Gecer, E. N.; Erenler, R. J Chem Soc Pakistan 2022, 44 (6), 610-617.
- Gecer, E. N.; Erenler, R.; Temiz, C.; Genc, N.; Yildiz, I. Particul Sci Technol 2022, 40 (1), 50-57.
- Karan, T.; Erenler, R.; Bozer Moran, B. Z Naturforsch C J Biosci 2022, 77 (7-8), 343-350.
- Sahin Yaglioglu, A.; Erenler, R.; Gecer, E. N.; Genc, N. J Inorg Organomet Polym Mater 2022, 32, 3700-3707.
- Erenler, R.; Chaoui, R.; Yildiz, I.; Genc, N.; Gecer, E. N.; Temiz, C.; Akkal, S. Trends Sci 2023, 20 (10), 6105-6105.
- Erenler, R.; Gecer, E. N.; Hosaflioglu, I.; Behcet, L. Biochem Bioph Res Co 2023.
- Erenler, R.; Gecer, E. N.; Hosaflioglu, I.; Behcet, L. Biochem Bioph Res Co 2023, 659, 91-95.
- Topçu, G.; Erenler, R.; Çakmak, O.; Johansson, C. B.; Çelik, C.; Chai, H.-B.; Pezzuto, J. M. Phytochemistry 1999, 50 (7), 1195-1199.
- Elmastas, M.; Ozturk, L.; Gokce, I.; Erenler, R.; Aboul-Encin, H. Y. Anal Lett 2004, 37 (9), 1859-1869.
- Demirtas, I.; Erenler, R.; Elmastas, M.; Goktasoglu, A. Food Chem 2013, 136 (1), 34-40.
- Sahin Yaglioglu, A.; Akdulum, B.; Erenler, R.; Demirtas, I.; Telci, I.; Tekin, S. Med Chem Res 2013, 22 (6), 2946-2953.
- Erenler, R.; Pabuccu, K.; Yaglioglu, A. S.; Demirtas, I.; Gul, F. Z Naturforsch C J Biosci 2016, 71 (3-4), 87-92.
- Aksit, H.; Çelik, S. M.; Sen, Ö.; Erenler, R.; Demirtas, I.; Telci, I.; Elmastas, M. Rec Nat Prod 2014, 8 (3), 277-280.
- Bayir, B.; Gündüz, H.; Usta, T.; Şahin, E.; Özdemir, Z.; Kayır, Ö.; Sen, Ö.; Akşit, H.; Elmastaş, M.; Erenler, R. J New Results Sci 2014, 6 (6), 44-50.
- Erenler, R.; Yilmaz, S.; Aksit, H.; Sen, O.; Genc, N.; Elmastas, M.; Demirtas, I. Rec Nat Prod 2014, 8 (1), 32-36.
- Kaya, G.; Karakaya, R.; Tilgel, E.; Sandikci, M.; Yucel, E.; Cicek, G.; Kayır, O.; Aksit, H.; Telci, I.; Guzel, A. J New Results Sci 2014, 7 (7), 1-6.
- Elmastas, M.; Erenler, R.; Isnac, B.; Aksit, H.; Sen, O.; Genc, N.; Demirtas, I. Nat Prod Res 2016, 30 (3), 299-304.
- Erenler, R.; Cakmak, O. J Chem Res F2004, (8), 566- 569.
- Erenler, R.; Biellmann, J. F. Tetrahedron Lett 2005, 46 (34), 5683-5685.
- Cakmak, O.; Erenler, R.; Tutar, A.; Celik, N. J Org Chem 2006, 71 (5), 1795-1801.

30. Erenler, R.; Biellmann, J. F. *J Chin Chem Soc* 2007, 54 (1), 103-108.
31. Erenler, R.; Uno, M.; Goud, T. V.; Biellmann, J. F. *J Chem Res* 2009, 2009 (7), 459-464.
32. Lu, J.; Maezawa, I.; Weerasekara, S.; Erenler, R.; Nguyen, T. D. T.; Nguyen, J.; Swisher, L. Z.; Li, J.; Jin, L. W.; Ranjan, A.; Srivastava, S. K.; Hua, D. H. *Bioorgan Med Chem Lett* 2014, 24 (15), 3392-3397.
33. Koyuncu, O.; Yaylacı, Ö. K.; Özgüşi, K.; Sezer, O.; Öztürk, D. *Plant Syst Evol* 2013, 299 (10), 1839-1847.
34. Erenler, R.; Yildiz, I.; Aydin, A.; Genc, N. *Medical Oncology* 2022, 39 (8), 116.
35. Di Giorgio, C.; Delmas, F.; Tueni, M.; Cheble, E.; Khalil, T.; Balansard, G. *J Altern Complement Med* 2008, 14 (2), 157-162.
36. Erenler, R.; Sen, O.; Aksit, H.; Demirtas, I.; Yaglioglu, A. S.; Elmastas, M.; Telci, İ. *J Sci Food Agr* 2016, 96 (3), 822-836.
37. Erenler, R.; Adak, T.; Karan, T.; Elmastas, M.; Yildiz, I.; Aksit, H.; Topcu, G.; Sanda, M. A. *The Eurasia Proceed Sci Tech Eng Math* 2017, 1, 139-145.
38. Erenler, R.; Meral, B.; Sen, O.; Elmastas, M.; Aydin, A.; Eminagaoglu, O.; Topcu, G. *Pharm Biol* 2017, 55 (1), 1646-1653.
39. Guzel, A.; Aksit, H.; Elmastas, M.; Erenler, R. *Pharmacogn Mag* 2017, 13 (50), 316.
40. Elmastas, M.; Celik, S. M.; Genc, N.; Aksit, H.; Erenler, R.; Gulcin, İ. *Int J Food Prop* 2018, 21 (1), 374-384.
41. Dede, E.; Genc, N.; Elmastas, M.; Aksit, H.; Erenler, R. *Nat Prod J* 2019, 9 (3), 238-243.
42. Erenler, R.; Nusret, G.; Elmastaş, M.; Eminagaoglu, Ö. *Turk J Biodiv* 2019, 2 (1), 13-17.
43. Erenler, R.; Hosaflioglu, I. *Mater Today Commun* 2023, 35, 105863.
44. Istifli, E. S. *Molecules* 2021, 26 (10), 2981.
45. Erenler, R.; Ojelade, R. A.; Karan, T.; Gecer, E. N.; Genc, N.; Yaman, C. *Inorg Chem Commun* 2023, 158, 111623.
46. Gecer, E. N. *Green Process Synth* 2023, 12 (1), 20228126.
47. Ajitha, B.; Reddy, Y. A. K.; Reddy, P. S.; Suneetha, Y.; Jeon, H.-J.; Ahn, C. W. *J Mol Liq* 2016, 219, 474-481.
48. Kumar, P. V.; Pammi, S.; Kollu, P.; Satyanarayana, K.; Shameem, U. *Ind Crop Prod* 2014, 52, 562-566.
49. Gecer, E. N.; Erenler, R. *J Indian Chem Soc* 2023, 100 (5), 101003.
50. Karan, T.; Erenler, R.; Gonulalan, Z.; Kolemen, U. *Chem Pap* 2024, 78 (1), 473-481.
51. Karan, T.; Gonulalan, Z.; Erenler, R.; Kolemen, U.; Eminagaoglu, O. *J Mol Struct* 2024, 1296, 136836.
52. Yaman, C.; Erenler, R.; Atalar, M. N.; Adem, Ş.; Çalışkan, U. K. *Brazilian Archives of Biology and Technology* 2024, 67, e24230043.
53. Hadjra, H.; Yamina, B.; Soulef, K.; Erenler, R. *Jordan J Biol Sci* 2023, 16 (4), 665-672.
54. Khodja, E. A. T.; Abd El Hamid Khabtane, R. A.; Benouchenne, D.; Bensaad, M. S.; Bensouici, C.; Erenler, R. *J Tradit Chin Med* 2023, 43 (2), 252.
55. Guemidi, C.; Ait Saada, D.; Ait Chabane, O.; Elmastas, M.; Erenler, R.; Yilmaz, M. A.; Tarhan, A.; Akkal, S.; Khelifi, H. *Food Science & Nutrition* 2024.